Aalborg Universitet

AALBORG UNIVERSITY
DENMARK

A Dual-Polarized Linear Antenna Array with Improved Isolation Using A Slotline-Based 180° Hybrid for Full-Duplex Applications

Zhang, Yiming; Zhang, Shuai; Li, Jia-Lin; Pedersen, Gert F.

A Dual-Polarized Linear Antenna Array with Improved Isolation Using A Slotline-Based 180° Hybrid for Full-Duplex Applications

Yi-Ming Zhang, *Student Member*, *IEEE*, Shuai Zhang, Jia-Lin Li, and Gert Frølund Pedersen

Abstract—**This paper presents a simple and compact dual-polarized linear antenna array characterizing high inter-port isolation for in-band full-duplex communications. By using the symmetrically shared-interface configuration integrated with a 180° hybrid, the self-interference resulting from the impedance mismatching between the antenna and feeding network, and the coupling among the antenna elements can be well suppressed theoretically. Furthermore, to achieve the high isolation in practice among a wide frequency band, a slotline-based 180° hybrid is proposed and studied, which features a high isolation between the sum and differential ports. For further verification, a demonstrator of a 1×4 array centered at 5.0 GHz is developed and fabricated. The measurements denote that the shared -10 dB impedance bandwidth of the two ports is from 4.75 to 5.18 GHz, and the inter-port 50 dB-isolation bandwidth is from 4.55 to 5.66 GHz (over 21.7 %).**

Index Terms— **In-band full duplex, self-interference, dual polarization, 180° hybrid, slotline.**

I. INTRODUCTION

To realize a full-duplex system where the spectrum efficiency can be doubled compared to those using half-duplex operations, an essential work is the suppression of the self-interference caused by the leakage from the transmitter to the local receiver [1]-[9]. As mentioned in [7]-[9], the isolation achieved at the antenna level should be as high as possible to ease the burdens of the subsequent analog or digital cancellations and obtain a total level of over 100-dB isolation. Seeing that certain isolation can be observed between orthogonal polarizations naturally, using dual-polarized antennas with isolation-improved techniques is valuable for the in-band full-duplex communications [4]-[9].

By designing well-organized dual-polarized antennas, high inter-port isolation can be achieved for single-antenna scenarios [6]-[10]. For instance, in [8] and [9], differential-fed

Yi-Ming Zhang and Jia-Lin Li are with the School of Physics, University of Electronic Science and Technology of China, Chengdu 610054, China. Yi-Ming Zhang is also with the Antenna, Propagation and Millimeter-wave Systems (APMS) Section, Aalborg University, Aalborg 9220, Denmark (e-mail: ymzhang@std.uestc.edu.cn, yiming@es.aau.dk, jialinli@uestc.edu.cn).

Shuai Zhang and Gert Frølund Pedersen are with the Antenna, Propagation and Millimeter-wave Systems (APMS) Section, Aalborg University, Aalborg 9220, Denmark (e-mail: sz@es.aau.dk, gfp@es.aau.dk).

dual-polarized antennas were investigated at 2.4 GHz, where three- or four-port antenna elements using the rat-race hybrids were employed for realization. The inter-port isolations were higher than 70 dB within a narrow band around 50 MHz. The radiation efficiencies of the antennas were 45-55% within the band. However, for antenna-array systems, the complicated mutual coupling among the antenna elements makes it difficult to realize a high inter-port isolation level [11]-[13]. In [12], a 4×4 dual-polarized antenna array centered at 24.5 GHz was designed. Despite that aperture-coupled patch antennas featuring high isolation were utilized, the realized inter-port isolation of the array was around 35 dB from 22 to 26.5 GHz. Besides, using electromagnetic-bandgap structure or defected ground structure can suppress the mutual coupling within antenna arrays, at the cost of bulky systems [14]-[17].

In this work, a dual-polarized linear antenna array is studied for full-duplex communications. By integrating with the proposed slotline-based 180° hybrid, the leakage from the transmitter to the local receiver can be well canceled over a wide frequency band. The proposed architecture features simplicity, reciprocity, compact size, low profile as well as low insertion loss, making it valuable for antenna array-based full-duplex systems where high gain is required and strong mutual coupling should be suppressed, such as full-duplex base stations. The novelties of this work are as follows:

(1) Different from the conventional schemes using differential-fed antennas reported in [8] and [9], the proposed scenario uses the typical two-port patch antennas and one 180° hybrid to simultaneously realize common-mode feeding and differential-mode feeding. This will effectively decrease the complexity of the patch array feeding work;

(2) A compact slotline-based 180° hybrid is proposed, which features wideband impedance and high isolation responses. Besides, small magnitude and phase imbalances at the output ports are observed within a wide frequency band;

(3) The isolation level and isolation bandwidth of the proposed array are significantly enlarged by using the proposed slotline-based 180° hybrid.

II. PROPOSED ARRAY CONFIGURATION

Fig. 1 shows the configuration of the proposed scheme. The array includes a dual-polarized linear antenna array consisting of 45°-rotated square patches and a 180° hybrid. The only requirement for the dual-polarized element is that the

configuration should be symmetrical. Without loss of generality, the differential (Δ) and sum (Σ) ports of the hybrid are defined as the transmitting and receiving ports of the array, respectively. It is seen that when port 1 or port 2 is excited, vertical or horizontal polarization would be generated correspondingly. For this scheme, there are three kinds of self-interference, the reflection between the antenna and the hybrid, the coupling among antenna elements, and the leakage through the hybrid. With this architecture, the first two kinds of the mentioned self-interference can be well canceled as discussed below.
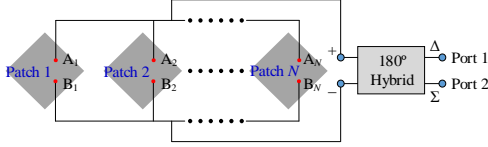

Fig. 1. Configuration of the proposed dual-polarized linear antenna array. The polarities "+" and "–" at the outputs of the hybrid are defined based on the differential port (Δ).
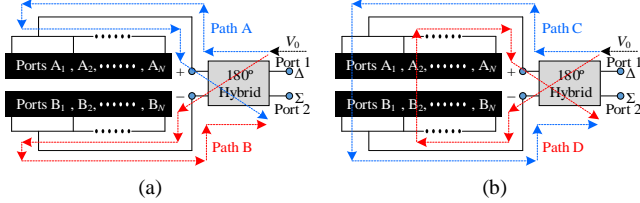

Fig. 2. Signal flow diagrams of the self-interference cancellations resulting from (a) the impedance mismatching of the antenna array and (b) the coupling among antenna elements.

For ease of analysis, the proposed array is considered as a combination of two subarrays marked as subarray A (from ports A_1 to A_N) and subarray B (from ports B_1 to B_N). As depicted in Fig. 2(a), defining the input voltage at port 1 as V_0, the output voltage $V_{total, 1}$ at port 2 through paths A and B can be estimated as

Path A: $V_A = |S_H| e^{-j\pi/2} \cdot S_A \cdot |S_H| e^{-j3\pi/2} \cdot V_0$ (1a)

Path B: $V_B = |S_H| e^{-j\pi/2} \cdot S_B \cdot |S_H| e^{-j\pi/2} \cdot V_0$ (1b)

Total voltage at port 2: $V_{total, 1} = V_A + V_B = 0$.   (1c)

where S_H is the transmission coefficient of the 180° hybrid, S_A and S_B are the reflection coefficients at the input interfaces of the two subarrays, respectively. Owing to the symmetrical configuration, it is found that $S_A = S_B$. Consequently, the voltage $V_{total, 1}$ is zero as shown in (1c). Using similar analysis, the total output voltage $V_{total, 2}$ at port 2 through paths C and D depicted in Fig. 2(b) can be estimated, expressed as

Path C: $V_C = |S_H| e^{-j\pi/2} \cdot C_{BA} \cdot |S_H| e^{-j\pi/2} \cdot V_0$ (2a)

Path D: $V_D = |S_H| e^{-j\pi/2} \cdot C_{BA} \cdot |S_H| e^{-j3\pi/2} \cdot V_0$ (2b)

Total voltage at port 2: $V_{total, 2} = V_C + V_D = 0$.   (2c)

where C_{BA} is the coupling coefficient between the subarray A and subarray B. Note that the self-coupling within the subarray A or subarray B is also canceled since it can be considered as a part of the reflection signal and has been analyzed based on Fig. 2(a), and thus are not detailed here for brevity. Furthermore, assuming that a high isolation level between the sum and differential ports of the 180° hybrid can be obtained, a good self-interference suppression would be achieved according to the above discussions, leading to a high inter-port isolation.

III. DESIGN DESCRIPTION OF DEMONSTRATOR

A. Slotline-Based 180° Hybrid

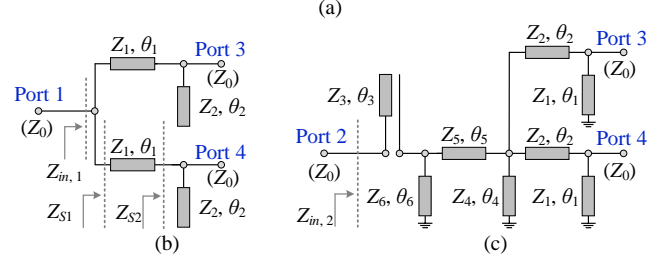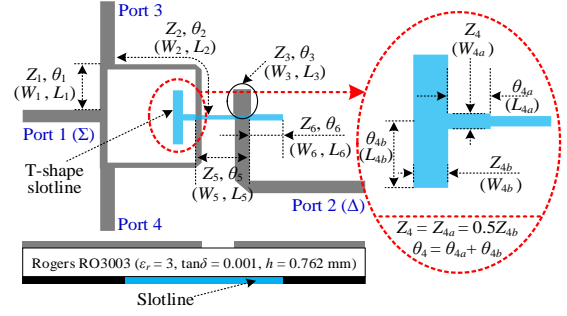Fig. 3. (a) Configuration of the proposed slotline-based 180° hybrid. Simplified circuits of the proposed 180° hybrid when (b) port 1 or (c) port 2 is excited.

As mentioned that the residue of the self-interference is the leakage through the 180° hybrid. In this work, a slotline-based 180° hybrid characterizing a wideband response with a high isolation level is presented. Please note that slotline-based microwave components have been studied widely, such as differential filters [18] and multi-layer transitions [19]. However, it is the first time to propose such a 180° hybrid where slotline is used to expand the bandwidth, reduce the magnitude/phase imbalance, and improve the isolation. As depicted in Fig. 3(a), the proposed hybrid includes a ring and a 50-Ω transmission line, which are connected by a half-wavelength slotline. All the electrical lengths refer to the center frequency f_0, which are $\theta_1 = 90°$, $\theta_2 = 180°$, $\theta_3 = 45°$, $\theta_4 = 90°$, $\theta_5 = 60°$, $\theta_6 = 30°$. The part with the electric length of θ_4 is realized by a T-shape structure for practice to increase the distance between the slotline and port 1, and reduce the coupling between the differential and sum ports. The characteristic impedance of the transmission lines will be determined based on the following discussions. According to the operational characteristics of the slotline, the phase difference between the two outputs would be 180° among a wide frequency band when port 2 is excited, while it should be always zero when port 1 is excited. For impedance matching, simplified equivalent circuits are constructed, as shown in Figs. 3(b) and 3(c). Subsequently, the input impedance $Z_{in, 1}$ at port 1 seen looking into the output interfaces versus frequency f can be given by

$$Z_{in,1} = Z_{S1}/2 \tag{3a}$$

$$Z_{S1} = Z_1 \frac{Z_{S2} + jZ_1 \tan(\theta_1 f / f_0)}{Z_1 + jZ_{S2} \tan(\theta_1 f / f_0)}, \quad Z_{S2} = \frac{Z_0 Z_2}{Z_2 + jZ_0 \tan(\theta_2 f / f_0)} \tag{3b}$$

Similarly, for the circuit illustrated in Fig. 3(c), we have

$$Z_{in,2} = \frac{Z_3}{j \tan(\theta_3 f / f_0)} + \frac{jZ_6 Z_{S3} \tan(\theta_6 f / f_0)}{Z_{S4} + jZ_6 \tan(\theta_6 f / f_0)} \tag{4a}$$

$$Z_{S3} = Z_5 \frac{Z_{S4} + jZ_5 \tan(\theta_5 f / f_0)}{Z_5 + jZ_{S4} \tan(\theta_5 f / f_0)}, \quad Z_{S4} = \frac{jZ_4 Z_{S5} \tan(\theta_4 f / f_0)}{Z_{S5} + j2Z_4 \tan(\theta_4 f / f_0)} \quad (4b)$$

$$Z_{S5} = Z_2 \frac{Z_{S6} + jZ_2 \tan(\theta_2 f / f_0)}{Z_2 + jZ_{S6} \tan(\theta_2 f / f_0)}, \quad Z_{S6} = \frac{jZ_0 Z_1 \tan(\theta_1 f / f_0)}{Z_0 + jZ_1 \tan(\theta_1 f / f_0)} \quad (4c)$$

where $Z_{in,2}$ is the input impedance at the interface of port 2. Z_{S1}, Z_{S2}, Z_{S3}, Z_{S4}, Z_{S5}, and Z_{S6} are the input impedances as marked in Fig. 3. For impedance matching purpose, we have

$$Z_{in,1} = Z_{in,2} = Z_0. \quad (5)$$

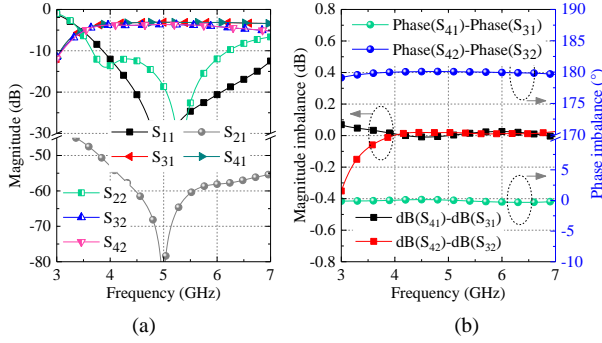Based on (3)-(5), all the characteristic impedance can be calculated and determined.

Fig. 4. Simulated transmission responses of the proposed slotline-based 180° hybrid. (a) S-parameters. (b) Magnitude and phase imbalances
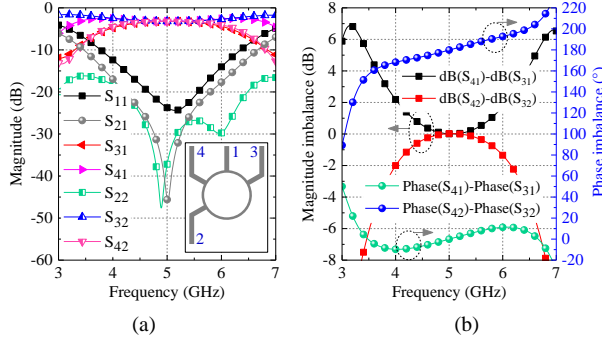

Fig. 5. (a) Simulated S-parameters of a typical rat-race hybrid centered at 5.0 GHz. (b) Magnitude and phase imbalances.

Consequently, a slotline-based 180° hybrid centered at 5.0 GHz is developed. The optimized physical sizes are (unit: mm): $L_1 = 7.0$, $L_2 = 17.4$, $L_3 = 3.8$, $L_{4a} = 2.0$, $L_{4b} = 8.0$, $L_5 = 7.0$, $L_6 = 4.3$, $W_1 = 1.0$, $W_2 = 0.8$, $W_3 = 2.3$, $W_{4a} = 0.6$, $W_{4b} = 0.8$, $W_5 = 0.3$, $W_6 = 0.6$. The full-wave simulated results (using CST STUDIO SUITE software) of the proposed hybrid are plotted in Fig. 4. It is found that a broadband isolation between the sum and differential ports from 4.0 to over 7.0 GHz is achieved referring to 50 dB. Within the studied frequency band, the errors in magnitude and phase imbalances are ±0.3 dB and ±1°, respectively. Fig. 5 illustrates the simulated results of the rat-race hybrid, a most common 180° hybrid, centered at 5.0 GHz for performance comparison, where the substrate Rogers RO3003 is used. It is found that the isolation of over 30 dB corresponds to a rather narrow bandwidth from 4.76 to 5.25 GHz, and degrades quickly as the frequency departs from the center frequency. As for the proposed hybrid, both the isolation level and the isolation bandwidth are significantly enhanced compared with those of the rat-race hybrid. Moreover, the errors in magnitude and phase imbalances of the proposed hybrid are much smaller over a wide frequency band.

B. 1×4 *microstrip antenna array*

For demonstration purpose, a 1×4 linear antenna array, centered at 5.0 GHz (around 4.9-GHz band) which is allocated for 5G systems, is designed as shown in Fig. 6(a). The array includes three stacked substrates. The radiation patches are printed on the top of substrate 1, and the feeding network is positioned on the bottom of substrate 3. A shared ground plane is inserted between substrates 2 and 3. The center distance d between adjacent elements is $0.5\lambda_0$, where λ_0 is the free space wavelength at 5.0 GHz. Fig. 6(b) illustrates the feeding networks of the 1×4 array using the conventional rat-race hybrid and without using any hybrids, marked as cases B and C respectively. For comparison purposes, full-wave simulations of cases A, B, and C are performed, where case A represents the proposed scheme. It is observed from Fig. 7 that within the impedance band, the isolation of case B has been only improved by 5 dB compared to that of case C, while the improvement for case A is 27 dB. This indicates that by using the proposed slotline-based 180° hybrid, the isolation level of the proposed array can be significantly enhanced as expected. Other simulated results of the antenna array integrated with the proposed 180° hybrid will be provided in the next section along with the measured results.
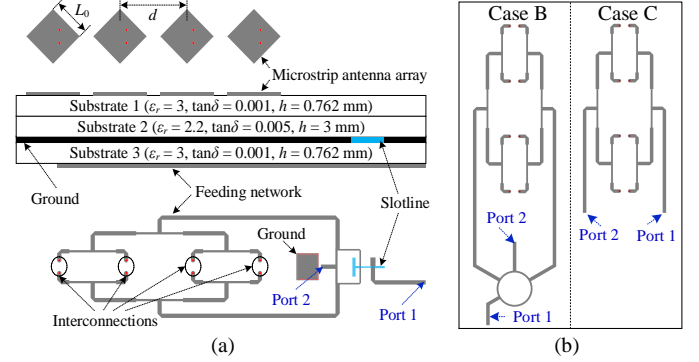

Fig. 6. Configurations of (a) the proposed 1×4 antenna array, and (b) the feeding networks of the 1×4 antenna array using the typical rat-race hybrid (case B) and the one without using any isolation improvements (case C).
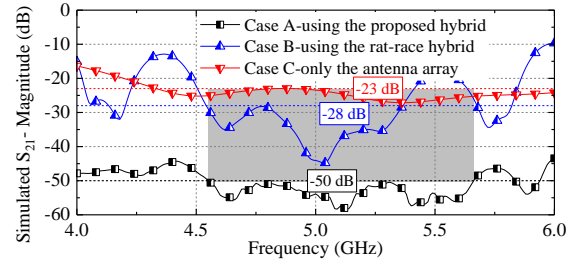

Fig. 7. Full-wave simulated transmission responses of the three cases, where case A is the proposed layout shown in Fig. 6(a).

IV. MEASUREMENTS

The developed 1×4 antenna array shown in Fig. 6(a) is fabricated and assembled, as photographed in Fig. 8. The metal screw positions have been carefully checked in simulations before the fabrication, which will not affect the performance of the antenna array. The transmission response of the array is measured in the lab environment by using the Agilent 85309B network analyzer, and the radiation performance is tested with the in-house SATIMO SG24L spherical near-field scanner.

When measuring one port, the other one was terminated with a 50-Ω load. As shown in Fig. 9, the measured impedance bandwidths of ports 1 and 2 are from 4.75 to 5.44 GHz, and from 4.69 to 5.18 GHz respectively, referring to $|S_{11}| \leq -10$ dB. A high isolation level of over 50 dB is obtained from 4.55 to 5.66 GHz with the percentage bandwidth of 21.7%. Good accordance between the measurements and the simulations is observed, except for some fluctuations mainly due to the practical errors and small environment reflections. The measured radiation patterns at 5.0 GHz are illustrated in Fig. 10. Excellent correlation is observed between the measured and simulated results. Besides, low cross-polarization levels are found, which are less than −30 dB and −24 dB corresponding to port 1 and port 2, respectively. The realized gains at the boresight direction are measured as illustrated in Fig. 11, which are higher than 11 dBi among the impedance bandwidths. The measured total efficiency is over 80% as also plotted in Fig. 11, exhibiting the low insertion-loss performance. The difference of the radiation between ports 1 and 2 is probably due to the differential feeding of the antenna when port 1 is excited.
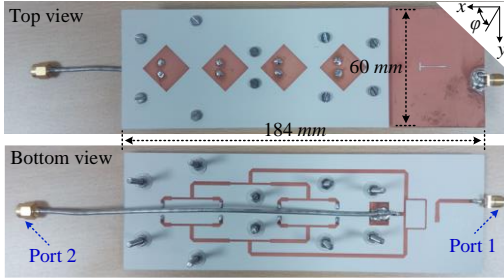

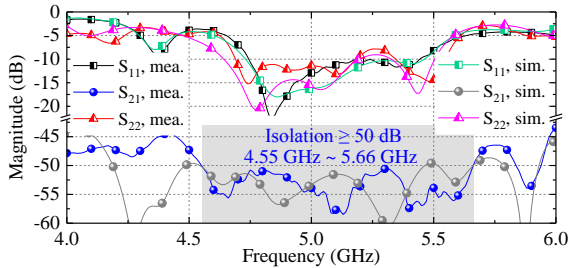Fig. 8. Photographs of the developed 1×4 dual-polarized antenna array.
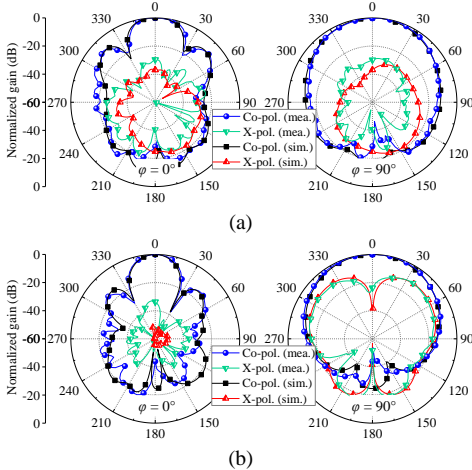

Fig. 9. S-parameters of the proposed 1×4 array.

Fig. 10. Radiation patterns of the array at 5.0 GHz. (a) Port 1 and (b) Port 2 with the co-polarization of *y*- and *x*-directions, respectively.

Table I summarizes some recently published dual-polarized

antennas for comparison purpose. For these studies, in spite of some additionally isolation-improvement methods, the inter-port isolation did not achieve a high level (≥ 50 dB) within a wide band. As for the proposed array, both simulated and measured results denote that a high isolation level of over 50 dB is observed among a wide frequency band, exhibiting the well-designed self-interference cancellation response. Please note that all the inter-port isolation in the comparison is from the measured results. This is because some practical issues of implementing different techniques may severely distort the isolation, which should be considered. Moreover, the proposed configuration is simple and compact, which can be readily extended to large-scale linear antenna arrays with low insertion loss and high efficiency.
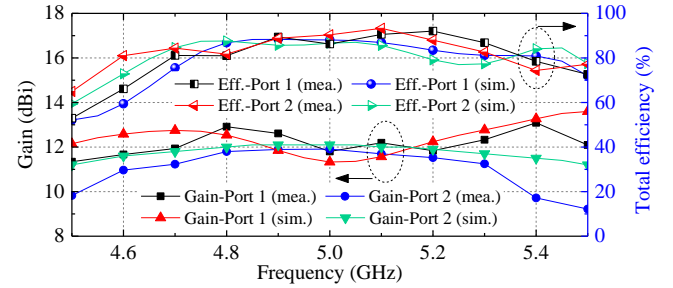

Fig. 11. Realized gain and total efficiency of the proposed array.

TABLE I
PERFORMANCE COMPARISONS AMONG SOME PUBLISHED DUAL-POLARIZED ANTENNAS AND THE PROPOSED DUAL-POLARIZED ANTENNA ARRAY

Ref./Year	[10]/2014	[11]/2008	[13]/2018	**This work**
Antenna configuration	Single element	2×4 4×4	2×2	1×4
Antenna type	Patch	Patch	Patch	Patch
Center distance among adjacent antennas	–	$0.73\lambda_0$ @5.5 GHz	$0.66\lambda_0$ @13.8 GHz	$0.5\lambda_0$ @5.0 GHz
Impedance bandwidth (GHz)	11.5~15.3	5.45~5.56	11.9~15.4	4.75~5.18 [a]
Improvement method of the isolation	SIRMHs [b]	Meandered feeding line	Q-SIW [c]	Hybrid-based feeding
Improvement level of the isolation	17 dB	14 dB	14 dB	27 dB
Inter-port isolation bandwidth (GHz)	11.0~16.0 (37%) (≥ 40 dB)	5.45~5.6 (3%) (≥ 40 dB)	11.9~14.8 (21.7%) (≥ 40 dB)	4.55~5.66 (21.7%) (≥ 50 dB)
Total efficiency	–	–	–	$\geq 80\%$ [d]

[a] denotes the shared band that $|S_{11}| \leq -10$ dB and $|S_{22}| \leq -10$ dB.
[b] denotes the substrate-integrated rows of metalized via holes.
[c] denotes the quasi-substrate integrated waveguide.
[d] denotes the measured total efficiency among the shared impedance band.

V. CONCLUSION

In this letter, a dual-polarized linear antenna array using shared-interface configuration is presented and studied for in-band full-duplex communications. By integrating with the proposed slotline-based 180° hybrid featuring a high isolation level between the sum and differential ports, the self-interference within the array can be well canceled. The simulated and measured results indicate that the presented array characterizes a high inter-port isolation level, leading it valuable and attractive for full-duplex applications.

REFERENCES

[1] F. Chen, R. Morawski, and T. Le-Ngoc, "Self-interference channel characterization for wideband 2×2 MIMO full-duplex transceivers using dual-polarized antennas," *IEEE Trans. Antennas Propag.*, vol. 66, no. 4, pp. 1967-1976, Apr. 2018.

[2] K. Iwamoto, M. Heino, K. Haneda, and H. Morikawa, "Design of an antenna decoupling structure for an inband full-duplex collinear dipole array," *IEEE Trans. Antennas Propag.*, vol. 66, no. 7, pp. 3763-3768, Jul. 2018.

[3] P. V. Prasannakumar, M. A. Elmansouri, and D. S. Filipovic, "Broadband reflector antenna with high isolation feed for full-duplex applications," *IEEE Trans. Antennas Propag.*, vol. 66, no. 5, pp. 2281-2290, May 2018.

[4] X. Wang, W. Che, W. Yang, W. Feng, and L. Gu, "Self-interference cancellation antenna using auxiliary port reflection for full-duplex application," *IEEE Antennas Wireless Propag. Lett.,* vol. 16, pp. 2873-2876, 2017.

[5] M. Kashaniafard, and K. Sarabandi, "Directional full-duplex rf booster for 2450 MHz ISM band," *IEEE Trans. Antennas Propag.*, vol. 65, no. 1, pp. 134-141, Jan. 2017.

[6] M. Heino, S. N. Venkatasubramanian, C. Icheln, and K. Haneda, "Design of wavetraps for isolation improvement in compact in-band full-duplex relay antennas," *IEEE Trans. Antennas Propag.*, vol. 64, no. 3, pp. 1061-1070, Mar. 2016.

[7] D. Korpi, M. Heino, C. Icheln, K. Haneda, and M. Valkama, "Compact inband full-duplex relays with beyond 100 dB self-interference suppression: enabling techniques and field measurements," *IEEE Trans. Antennas Propag.*, vol. 65, no. 2, pp. 960-965, Feb. 2017.

[8] H. Nawaz, and I. Tekin, "Dual-polarized, differential fed microstrip patch antennas with very high interport isolation for full-duplex communication," *IEEE Trans. Antennas Propag.*, vol. 65, no. 12, pp. 7355-7360, Dec. 2017.

[9] H. Nawaz, and I. Tekin, "Double-differential-fed, dual-polarized patch antenna with 90 dB interport RF isolation for a 2.4 GHz in-band full-duplex transceiver," *IEEE Antennas Wireless Propag. Lett.,* vol. 17, no. 2, pp. 287-290, Feb, 2018.

[10] S.-J. Li, J. Gao, X. Cao, Z. Zhang, and D. Zhang, "Broadband and high-isolation dual-polarized microstrip antenna with low radar cross section," *IEEE Antennas Wireless Propag. Lett.,* vol. 13, pp. 1413-1416, Feb, 2014.

[11] I. Ac´imovic´, D. A. McNamara, and A. Petosa, "Dual-polarized microstrip patch planar array antennas with improved port-to-port isolation," *IEEE Trans. Antennas Propag.*, vol. 56, no. 11, pp. 3433-3439, Nov. 2008.

[12] A. I. Md and C. K. Nemai, "A 4×4 dual-polarized mm-wave ACMPA array for a universal mm-wave chipless RFID tag reader," *IEEE Trans. Antennas Propag.*, vol. 63, no. 4, pp. 1633–1640, Apr. 2015.

[13] W. Wang, J. Wang, A. Liu, and Y. Tian, "A novel broadband and high-isolation dual-polarized microstrip antenna array based on quasi-substrate integrated waveguide technology," *IEEE Trans. Antennas Propag.*, vol. 66, no. 2, pp. 951-956, Feb. 2018.

[14] L. Yang, M. Fan, F. Chen, J. She, and Z. Feng, "A novel compact electromagnetic-bandgap structure and its applications for microwave circuits," *IEEE Trans. Microw. Theory Tech.*, vol. 53, no. 1, pp. 183-190, Jan. 2005.

[15] L. Yang, M. Fan, F. Chen, J. She, and Z. Feng, "Reduction of mutual coupling in planar multiple antenna by using 1-D EBG and SRR structures," *IEEE Trans. Antennas Propag.*, vol. 63, no. 9, pp. 4194-4198, Sep. 2015.

[16] I. Dioum, A. Diallo, S. M. Farssi, and C. Luxey, "A novel compact dual-band LTE antenna-system for MIMO operation," *IEEE Trans. Antennas Propag.*, vol. 62, no. 4, pp. 2291-2296, Apr. 2014.

[17] X. Wang, W. Che, W. Yang, W. Feng, and L. Gu, "An integrated dual MIMO antenna system with dual-function GND-plane frequency-agile antenna," *IEEE Antennas Wireless Propag. Lett.,* vol. 17, no. 1, pp. 142-145, Jan. 2018.

[18] X. Guo, L. Zhu, K.-W. Tam, and W. Wu, "Wideband differential bandpass filters on multimode slotline resonator with intrinsic common-mode rejection," *IEEE Trans. Microw. Theory Tech.*, vol. 63, no. 5, pp. 1587-1594, May 2015.

[19] X. Guo, L. Zhu, J. Wang, and W. Wu, "Wideband microstrip-to-microstrip vertical transitions via multiresonant modes in a slotline resonator," *IEEE Trans. Microw. Theory Tech.*, vol. 63, no. 6, pp. 1902-1909, Jun. 2015.